J Mater Sci: Mater Med (2007) 18:829–837
DOI 10.1007/s10856-006-0001-5

Density functional calculations of the properties of silicon-substituted hydroxyapatite

H. F. Chappell · P. D. Bristowe

Received: 7 April 2005 / Accepted: 8 December 2005 / Published online: 19 December 2006

Abstract Ab initio density functional plane-wave calculations are performed on silicon-substituted hydroxyapatite (SiHA). Formation energies are obtained for the substitution of a phosphorus atom by a silicon atom in each of the six phosphate groups of the unit cell in turn. It is found that the co-removal of a hydroxyl group to maintain charge neutrality is energetically favourable and the calculated unit cell volumes for the single silicon substitutions agree extremely well with experimental observation. The substitution of a second silicon atom in the unit cell is found to be almost as energetically favourable as the first (and on one site more favourable) and there can be an attractive interaction between the two Si substituents when they are closely separated. However, experimental observation suggests that for this concentration of silicon a phase transformation to a different structure occurs which, because of the imposed boundary conditions, could not be accessed in the calculations. The density of states of the SiHA indicates that new states are introduced deep into the valence band and the band gap decreases by 1.6 eV compared to phase-pure HA. No new states are introduced into the band gap indicating that the Si incorporation does not make the material inherently electrically active. Furthermore a population analysis shows that the Si impurity has only a small effect on the neighbouring ionic charge.

H. F. Chappell (✉) · P. D. Bristowe
Department of Materials Science and Metallurgy, University of Cambridge, Pembroke Street, Cambridge CB2 3QZ, UK
e-mail: hc263@cam.ac.uk

1 Introduction

Hydroxyapatite, $Ca_{10}(PO_4)_6(OH)_2$, is similar in composition to the main inorganic mineral component of all mammalian hard tissue, primarily bone and tooth enamel [1]. It is relatively simple to manufacture synthetic, biologically similar compounds, some of which have already proven extremely useful in medical applications because of their innate bioactivity. For example, hydroxyapatite–polyethylene composites have been employed with great success, in middle ear prostheses [2]. Generally, a bioactive material is one that provokes a biological response from its host; in this case the response is bone apposition onto the material's surface [2]. However, hydroxyapatite is never found in its pure form in vivo, for example it has been reported that tooth enamel has many OH^- ions substituted by CO_3^{2-} ions. This accounts for between 5 and 10% of the total CO_3^{2-} content in this particular tissue and is one of the two most common ion substitutions, PO_4^{3-} by CO_3^{2-} and OH^- by CO_3^{2-}. These forms are called B-type and A-type hydroxyapatite, respectively, with the B-type being the most common biologically [3]. Additionally, experimental research has shown that while pure hydroxyapatite is innately bioactive it can be improved substantially by introducing defects and ion substitutions into the crystal lattice [4]. Substituted apatites are found in all mammalian hard tissue and are thought to confer, amongst other things, greater strength. For example, the replacement of the OH^- groups by F^- to form the less soluble fluorapatite, increases resistance to decay in tooth enamel [1, 5, 6]. Indeed, it is thought that hydroxyapatite (HA) effectively constitutes the mineral reservoir for the body, ions being released by its dissolution.

For many years now HA has been used variously in medical applications. These include porous hydroxyapatite ceramic implants, metallic implants with hydroxyapatite surface coatings and inorganic ceramic-polymer fillers [7]. Notably, a hydroxyapatite-reinforced polyethylene composite material known as HAPEX™ has been created [2]. Nevertheless, it should be noted that HA is not the only bioactive substance to be used in these types of applications; silicate glasses are another major component of device application and research. Manifestly, the success of these silicon-based substitutes has led to both experimental and theoretical work on the introduction of silicon into the hydroxyapatite crystal structure [7, 8].

2 Hydroxyapatite and silicon

Recently, experimental work on HA and its substituted counterparts such as silicon-doped HA (SiHA) has focused on finding a measurable indicator of bioactivity. In 1998, Wen and colleagues looked at the grain boundaries in dental hydroxyapatite and suggested that dissolution or mineralization may start from dislocations and defects at these boundaries [9]. Within synthetically produced hydroxyapatite these boundaries are ''clean'' with few defects or voids. However, it was noted that biological apatite is much more amorphous in nature with complicated structures at the junction of multiple grain boundaries where pockets of protein material can accumulate [9]. More recently a study was undertaken to investigate grain boundary structures in hydroxyapatite and silicon-substituted hydroxyapatite [10]. It was revealed that while there was no significant difference in dislocation density between HA and SiHA there was certainly an increase in triple junctions with increased silicon doping. If as the previous work suggested, dislocations were the starting point for dissolution then these differences in grain boundaries would account for and lead to the elucidation of bioactivity as a measurable effect [10].

In a piece of follow-up work, changes in HA and SiHA crystal structure were investigated in vivo in order to detail the predominant sites of dissolution [11]. The results showed categorically that dissolution does occur preferentially from grain boundaries and triple junctions. Additionally, at triple junctions, it was the smallest grains that showed the greatest dissolution, suggesting that a decrease in grain size would lead to increased solubility and hence greater bioactivity. It is of particular interest to note that after sintering, SiHA has been shown to have a much finer grain structure than phase-pure HA [12] suggesting that silicon inhibits grain growth. These smaller grains in SiHA and the increased number of triple junctions make SiHA a real and important candidate for enhanced bioactive products [11]. Indeed, silicon-substituted calcium phosphate products for synthetic bone grafts, have already been produced [13].

Silicon has now become a major focus for research due to various studies exposing its critical involvement in bone growth. Conclusive evidence of silicon's role was first provided in the 1970s when microprobe studies showed silicon to be localised in bone-growth areas in young rats and mice, with concentrations of up to 0.5 wt% silicon in these sites [14]. Additionally, in 1999, it was reported that the deterioration in osteoblast function and growth, in cases of osteoporosis and osteopenia, was related to a decrease in biologically available silicon [15].

The more recent work utilised in vivo procedures to investigate the nature of bone ingrowth on hydroxyapatite and silicon-doped hydroxyapatite implants [16]. Fluorochrome labels revealed sites of active bone deposition for both HA and SiHA from 1 to 3 weeks after implantation [16]. Indeed, with SiHA, new bone was found to deposit directly onto the implant surface without any form of fibrous encapsulation; a risk with less bioactive implants. These results showed that bone developed normally on and near the doped implants as well as on the phase-pure implants. Additionally, histomorphometry experiments carried out by this group showed that the silicon-doped hydroxyapatite implants had the greatest rates of bone in-growth and on-growth but also, they showed a faster rate of apposition which could be indicative of a potentially much more useful implant material [16].

Concerns about crystal structure changes in the HA on incorporation of silicon have been addressed by several experimental groups [15, 16]. Importantly it has been found that the incorporation of silicon into the crystal has little effect on the crystal structure. X-ray diffraction studies revealed that the intensity, width and position of peaks for 0.4, 0.8 and 1.5 wt% silicon HA were very similar to those of phase-pure hydroxyapatite [17]. Additionally, the Ca/P + Si ratio remains at the phase-pure value of 1.67, showing that silicon substitutes for phosphorus atoms. This has been confirmed using XPS analysis [12, 15]. Although there are no dramatic changes in the crystal structure it should be noted that increasing the silicon content of the crystal does produce a slight change in the lattice parameters [10]. Recent experimental work has shown that there is a systematic increase in the *c*-lattice parameter and a concomitant increase in cell

volume with increasing silicon content [10]. It is important to recognise that the silicate has a formal charge of –4, compared to –3 for the phosphate group. In compensating for this excess negative charge it has been found experimentally that, on average, one hydroxyl group leaves the crystal for every silicon substitution.

It is this interest in silicon doped HA that has led to the study reported here. Computational methods are well placed to offer insight into changes in crystal structures at the atomic level and have been used to investigate the formation energy of phosphorus substitution by silicon in the bulk hydroxyapatite unit cell. The formation energy of a second silicon substitution in the unit cell at differing phosphate positions has also been calculated. For each substitution, one hydroxyl group was removed in order to maintain the charge neutrality of the cell. It is noted that incorporation of a single Si atom with a hydroxyl vacancy into the HA unit cell corresponds to an effective composition of 2.8 wt% Si in the bulk crystal. The effects of silicon substitution on the electronic properties of the material such as band structure, density of states and ionic charges are also described.

3 Computational methods and models

The calculations were performed using the CASTEP code which is an ab initio program that allows ground state energies to be calculated accurately for atomic systems using the principles of Density Functional Theory (DFT) [18]. The concepts and principles involved in DFT simulations have been detailed elsewhere and have been used successfully for many years on an extensive range of systems [18, 19]. The code uses a plane wave basis set and ultra-soft pseudopotentials [20] that model the interaction between the atomic cores and the valence electrons. This approach allows the core electron interactions to be simplified and only the valence–electron–atomic core interactions to be treated explicitly. The plane wave basis set represents the valence electron orbitals and is limited by an imposed cut-off energy (E_{cut}), which was determined for each material used in this study before the main calculations were undertaken. The total energy was calculated with increasing cut-off energies until convergence was achieved. The convergence of total energy not only depends on E_{cut} but also on the k-point sampling of the Brillouin Zone [21]. Therefore, k-point separation was investigated in a similar manner to E_{cut}. A k-point grid size of $2 \times 2 \times 3$ was chosen for all the HA relaxations. These preliminary calculations were performed not only on HA but also on various other elements and related compounds used to determine the formation energies as described below. All the calculations were performed within the generalized gradient-approximation (GGA) and the PBE exchange-correlation potential was used throughout [22]. The electronic ground state was reached using a conjugate gradients algorithm [23] and the BFGS optimisation method [23] was used to relax the atomic structure. The perfect HA unit cell (obtained from the Materials Studio package [24]), which is hexagonal, contained 44 atoms and after relaxation the cell parameters were found to be $a = b = 9.479$ Å and $c = 6.850$ Å. These values agree with experimental measurements to within 0.5 %. Figure 1 shows two views of the phase-pure HA unit cell with the phosphate and hydroxyl groups labelled.

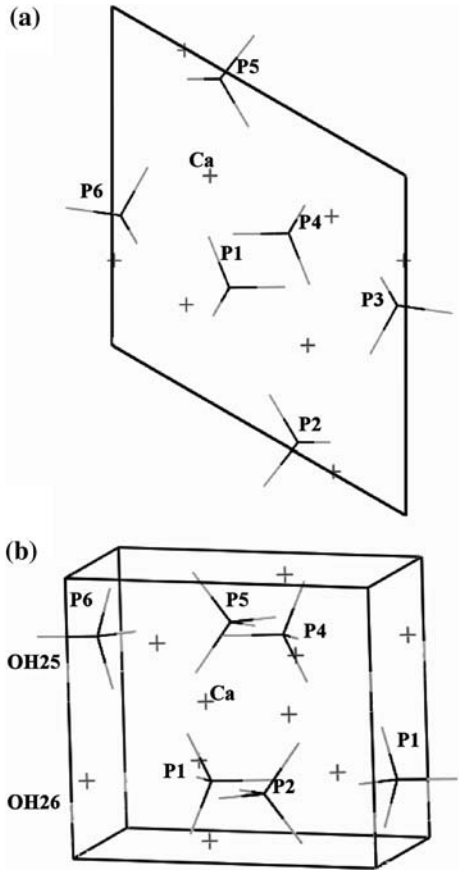

Fig. 1 The structure of phase-pure hydroxyapatite: (**a**) Hexagonal unit cell viewed down the [0001] c-axis. The unit cell dimensions are $a = b = 9.479$ Å, (**b**) perspective view with [0001] pointing into the paper. The c-axis dimension is 6.850 Å. The six phosphate groups are labelled P1–P6 and the two hydroxyl groups are OH25 and OH26. Calcium atoms are represented by crosses

The formation energy of a silicon substitutional impurity on a phosphorous site in a HA unit cell containing an hydroxyl vacancy is given by

$$E_{\text{form}} = E\{\text{Si}_\text{P}\text{HA} + V_{\text{OH}}\} - (E\{\text{HA} + V_{\text{OH}}\} - \mu_\text{P} + \mu_\text{Si}) \quad (1)$$

where $E\{\text{Si}_\text{p}\text{HA} + V_{\text{OH}}\}$ is the energy of the supercell with the silicon and missing hydroxyl group, and $E\{\text{HA} + V_{\text{OH}}\}$ is the energy of the OH-deficient pure HA unit cell. The chemical potentials of the substituted atom (P) and impurity atom (Si) are given by μ_P and μ_Si, respectively. In this work the chemical potentials are approximated by their 0 K energies per atom or molecule and their values are estimated using various chemical sources and sinks. In determining these potentials the aim is obtain the lowest values possible for that particular species. The choice of suitable sources and sinks depends on several factors: the range of commonly occurring oxides for the species concerned, their similarity to the actual components of synthetically produced HA, and ease of calculation. The chemical potentials of P and Si were obtained using the following sinks and sources: two polymorphs of elemental phosphorus (one monoclinic and the other orthorhombic), phosphorous oxide, phosphoric oxide, elemental silicon, quartz and cristobalite.

Initially, the total relaxed energy of the supercell, $E\{\text{Si}_\text{p}\text{HA} + V_{\text{OH}}\}$, was obtained from an *average* of the relaxed energies of the 12 different cells that can be generated when replacing one phosphate group with one silicate group in the presence of an hydroxyl vacancy. The energies for the 12 cells were similar, within 0.5 eV of each other, as shown in Table 1 and gave a reasonable average for $E\{\text{Si}_\text{p}\text{HA} + V_{\text{OH}}\}$ to use in the first instance.

4 Results and discussion

4.1 Substitution of a single Si atom

Calculation of the chemical potentials of Si and P using the various sources and sinks listed above lead to 30 different combinations of Eq. 1. Figure 2 illustrates the resulting Si formation energies, shown as diamonds, as a function of $\mu_\text{P} - \mu_\text{Si}$.

The figure indicates that a wide range of formation energies (about –13 to +15 eV) can be obtained by using the various combinations of μ_P and μ_Si. The plot is a straight line with unit gradient as expected from Eq. 1 and the point where it crosses the vertical axis corresponds to the Si-substitution energy in OH-deficient HA, that is $E\{\text{Si}_\text{p}\text{HA} + V_{\text{OH}}\} - (E\{\text{HA} + V_{\text{OH}}\})$, which has a constant value of 70.4 eV. It is therefore necessary to ask, which formation energy is the most appropriate? One possible way of determining a suitable formation energy is to use the lowest values for the variables in Eq. 1. In Fig. 2 the grey circular symbol on the OH-deficient series (plotted as diamonds) indicates the formation energy obtained from combining the lowest values of μ_P, –189.922 eV, and μ_Si, –118.867 eV, giving a value for E_{form} of –0.612 eV. But is this result reasonable given the chemistry of the materials it represents and the way synthetic SiHA is actually produced?

This particular combination of chemical potentials uses cristobalite as the source of silicon and phosphoric oxide as the sink for phosphorus. The experimental procedure for making synthetic SiHA employs a precipitation reaction of orthophosphoric acid, for the phosphate sink, and a silicon salt such as silicon acetate, for the silicon source [25]. Phosphoric oxide is the acid anhydride of orthophosphoric acid and thus our choice of sink for μ_P is identical to that of the

Table 1 Relaxed supercell energies and structural parameters resulting from the geometry optimization of 12 silicon-substituted HA unit cells in the presence of an hydroxyl vacancy

The unit cell notation is such that the first number indicates the hydroxyl group remaining and the last number is the substituted phosphorus atom. See Fig. 1 for the labelling scheme

Cell	Supercell energy (eV)	a (Å)	b (Å)	c (Å)	Cell volume (Å^3)	α (°)	β (°)	γ (°)
25P1	–22098.029	9.402	9.507	6.898	532.802	90.938	90.176	120.196
25P2	–22097.763	9.392	9.396	6.862	526.450	90.015	89.913	119.617
25P3	–22098.030	9.504	9.427	6.898	532.649	88.887	90.932	120.448
25P4	–22097.533	9.424	9.443	6.864	527.026	89.967	90.054	120.386
25P5	–22097.531	9.379	9.424	6.864	527.027	90.054	89.979	119.696
25P6	–22097.528	9.443	9.381	6.864	526.952	89.977	89.976	119.929
26P1	–22097.528	9.424	9.445	6.864	527.097	90.020	89.988	120.384
26P2	–22097.529	9.381	9.428	6.864	527.181	89.982	90.003	119.714
26P3	–22097.525	9.445	9.382	6.864	527.053	89.987	90.024	119.944
26P4	–22097.762	9.394	9.448	6.862	526.235	89.931	90.001	120.222
26P5	–22098.030	9.424	9.406	6.898	532.847	89.812	91.153	119.352
26P6	–22098.030	9.511	9.428	6.898	533.062	91.054	89.114	120.406

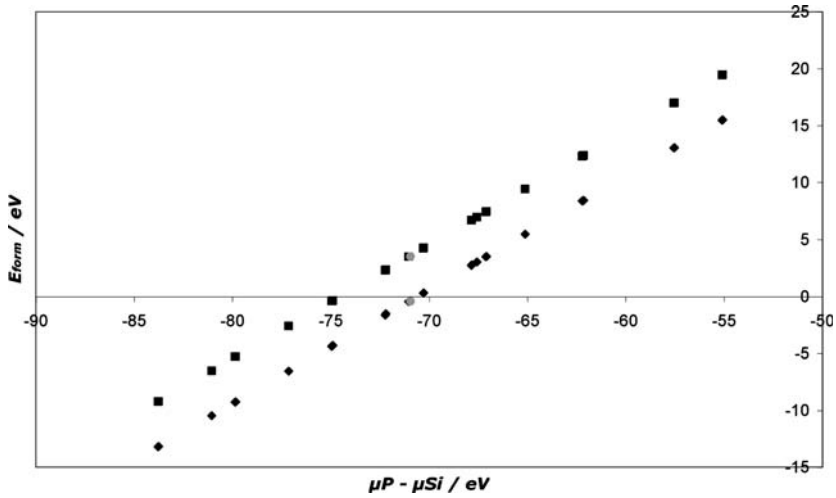

Fig. 2 Formation energy of the Si_P substitutional defect in HA as a function of $\mu_P - \mu_{Si}$. The diamonds represent the values of E_{form} calculated for a hydroxyl deficient unit cell (Eq. 1) and the squares represent the values of E_{form} calculated for a stoichiometric unit cell (Eq. 2). The grey circles at $\mu_P - \mu_{Si} = -71$ eV show the result obtained using the lowest chemical potentials in Eqs. 1, 2. Many of the data points have virtually identical values resulting in only 15 plotted rather than 30

experimentalists. However, our source of silicon is quite different and it is certainly not a silicon salt. Cristobalite is a solid at room temperature, identical in chemistry but different in structure to quartz. Experimentally, silicon acetate is the substance of choice, having a complicated structure with formula $C_8H_{12}O_8Si$. To determine μ_{Si} from this material would have required many additional calculations in order to find the energy of $C_8H_{12}O_8$. Each of these calculations would have introduced new uncertainties into the value of μ_{Si}. Therefore, although cristobalite is chemically quite different from the experimental source of silicon, it seems to be a reasonable choice given the computational demands and the need for accuracy. Thus, while the formation energy is not calculated in exactly the same manner as the experimental procedure, the value should be a reasonable estimate.

It can be seen that the resulting formation energy is negative but only slightly so. This indicates the relative ease with which silicon can be incorporated into HA and that OH-deficient SiHA is a stable phase, at least for the composition studied here (and of course ignoring thermodynamics and kinetics). Indeed, this would not be entirely surprising given that biologically, HA is never found in its phase-pure state but always with a high impurity level [26]. That is, the inorganic mineral component of bone resembles a highly substituted form of HA only. In addition, it is quite easy to produce low concentration (<1.5 wt% Si) SiHA material in the laboratory [26].

The formation energies determined so far have all been obtained using a value for $E\{Si_pHA + V_{OH}\}$ that is derived from a HA unit cell that has had a single silicon substitution made and one hydroxyl group removed. This method of performing the calculations was chosen because experimentally it has been observed using X-ray diffraction that the silicon-substituted unit cells have a reduction in the number of OH groups, while phase-pure HA has all the hydroxyls remaining. However, it was felt that perhaps an alternative calculation, with $E\{Si_pHA\}$ derived from a unit cell with both hydroxyl groups present, would produce an interesting comparison. That is, the total energy $E\{Si_pHA\}$ in Eq. 2 is that of a silicon-substituted unit cell with all the hydroxyl groups present

$$E_{form} = E\{Si_PHA\} - (E\{HA\} - \mu_P + \mu_{Si}). \quad (2)$$

The formation energy E_{form} obtained from this calculation using the lowest chemical potentials as before was +3.527 eV. This value is not only different from our original value of E_{form} but it is also significantly higher. This suggests that Si substitution with the hydroxyl groups present in the cell is less favourable than Si substitution in the charge neutral stoichiometric unit cell. Indeed, this result is encouraging, for experimentally this is exactly what is observed.

The square symbols shown in Fig. 2 illustrate the formation energies obtained using Eq. 2. It is seen that E_{form} shifts upwards for all values of $\mu_P - \mu_{Si}$ when a substituted unit cell that has all hydroxyl groups present is used. In fact, all values of E_{form} are increased by 4.14 eV, which highlights the importance of the formally charge neutral unit cell.

For completeness, after these initial calculations were carried out with an *average* value for $E\{Si_PHA + V_{OH}\}$, the formation energies were calculated separately for each of the 12 different substitutional combinations given in Table 1 using the lowest values for μ_P and μ_{Si}. Table 2 shows the results of these calculations where it is seen that the cells with lower ground-state energies and larger volumes (25P1,

Table 2 Formation energies, E_{form}, of the Si_P defect obtained from the 12 different substitutional combinations given in Table 1 and using the lowest values for μ_P and μ_{Si}

Cell	25P1	25P2	25P3	25P4	25P5	25P6	26P1	26P2	26P3	26P4	26P5	26P6
E_{form}/eV	–0.906	–0.640	–0.907	–0.410	–0.408	–0.405	–0.405	–0.405	–0.402	–0.639	–0.907	–0.907

25P3, 26P5, 26P6) correspond to the lowest defect formation energies. This indicates that there is a specific site preference within the unit cell for the silicon substitution and hydroxyl vacancy. Indeed, by referring to Fig. 1 it can be seen that the HA unit cell is essentially divided into a ''top'' and ''bottom'' half where the environments and substitution characteristics are similar.

Finally it is interesting to note the difference in cell volume of the Si-substituted HA structure with and without the hydroxyl vacancy. For example, for Si substitution made in the HA unit cell at phosphate position 4, the cell volume for the charge neutral cell is 527.027 $Å^3$. For the substituted unit cell with the hydroxyl group retained, the volume is 536.787 $Å^3$. These results can be compared to the experimentally measured cell volumes for SiHA which range from 527.799 to 528.143 $Å^3$ when 0.4–1.5 wt% Si is added [26]. The comparison further supports the X-ray diffraction evidence that the laboratory samples become deficient in hydroxyl groups when silicon is introduced.

4.2 Substitution of two Si atoms

Calculations were also performed to determine the formation energy of a second silicon substitution in the SiHA cell, i.e. the formation of a Si_P defect in the presence of an existing Si_P defect. To maintain charge neutrality, another hydroxyl group was removed for this substitution and the resulting composition was 5.6 wt% silicon. The example reference cell chosen arbitrarily for the second substitution was the 25P4 cell, as all the phosphate positions are approximately equivalent, and then additional substitutions were made in turn at positions P1, P2, P3, P5 and P6 along with the removal of the other hydroxyl group (OH25). The formation energies were determined according to Eq. 3 and are given in Table 3.

$$E_{form} = E\{2Si_PHA + 2V_{OH}\} - (E\{Si_PHA + 2V_{OH}\} - \mu_P + \mu_{Si}). \quad (3)$$

Table 3 Formation energies, E_{form}, of a second Si_P defect introduced into the 25P4 unit cell

Site of second substitution	E_{form} (eV)	Interaction energy (eV)
P1	–0.409	+0.004
P2	–0.323	–0.083
P3	–1.12	+0.718
P5	–0.348	–0.559
P6	–0.343	–0.564

The interaction energy between the two defects is obtained by subtracting the formation energy of the second substitution from that of the first

Table 3 shows that the formation energy for the second substitution is, with one exception, about the same as the first, which for the P4 position is –0.410 eV as shown in Table 2. The exceptional case is substitution on the P3 position where the formation energy is significantly lower (–1.12 eV). This implies that the second Si substitution is nearly as favourable as the first if not more so. Also shown are the interaction energies of the Si_P defects, obtained by subtracting the formation energy of the second substitution from the formation energy of the first substitution at the same position. Within the unit cell both silicon atoms are quite close to one another and it is seen that there is an attractive interaction between the Si_P defects for substitutions at P1 and P3 as the second energy is lower than the first. The substitutions at P2, P5 and P6, however, produce higher formation energies suggesting that there is a repulsive interaction between the Si_P defects in these positions. As the distance between the silicon atoms increases the second formation energy should tend to that of the first in the same position, i.e. the interaction energy should be zero.

What can be concluded from this discussion is that the second substitution is either more favourable or almost as favourable as the first. This suggests that the substitution would be likely to occur. However, it should be noted that in the laboratory silicon substitutions of 5.6 wt%, which is the composition of the doubly substituted unit cell, are never produced because of phase separation. Phase transformations involving reconstructions and large shape changes are not accessible in the present calculations. Our results are, however, a good indication of which substitutions

might occur in a much larger system with a much smaller *average* silicon concentration.

4.3 Electronic structures

The electronic structure of hydroxyapatite is of interest since there is some experimental evidence that charged surfaces of the crystal can lead to enhanced bioactivity [4]. The cause of these surface polarisations could be due, at least in part, to the presence of substituted impurities in the lattice that may accumulate near the surface. Before proceeding with surface segregation calculations it is necessary to understand the effect of impurity incorporation in the bulk crystal. Here we present information on how the electronic density of states changes in bulk HA when a P atom is substituted by a single Si atom in the lattice accompanied by a hydroxyl vacancy. Figure 3 compares the density of states of phase-pure HA with SiHA for substitution on the P1 site in a 26P1 cell.

The peaks were assigned to particular atomic orbitals by comparing to similar plots of the partial densities of states. It is seen that new peaks appear in the second valence band near –15 eV when Si is introduced and the band gap reduces from 5.5 to 3.9 eV. No new states are introduced into the band gap indicating that the Si incorporation does not make the material inherently electrically active. A Mulliken population analysis [27] was performed on the structures in order to obtain the ionic charges and bond populations. Note that although absolute values of these quantities were obtained, emphasis is placed on

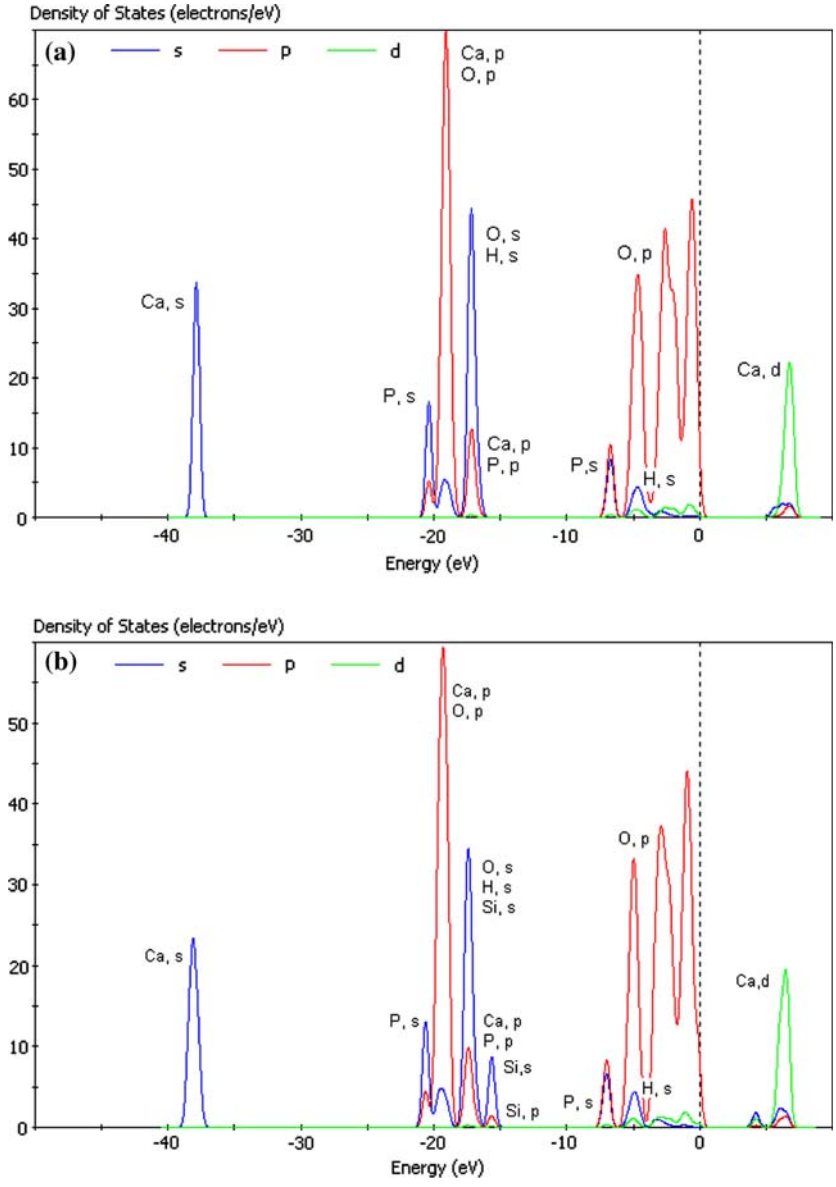

Fig. 3 Electronic density of states for (**a**) phase-pure HA and (**b**) Si-substituted HA. The dashed line indicates the valence band edge

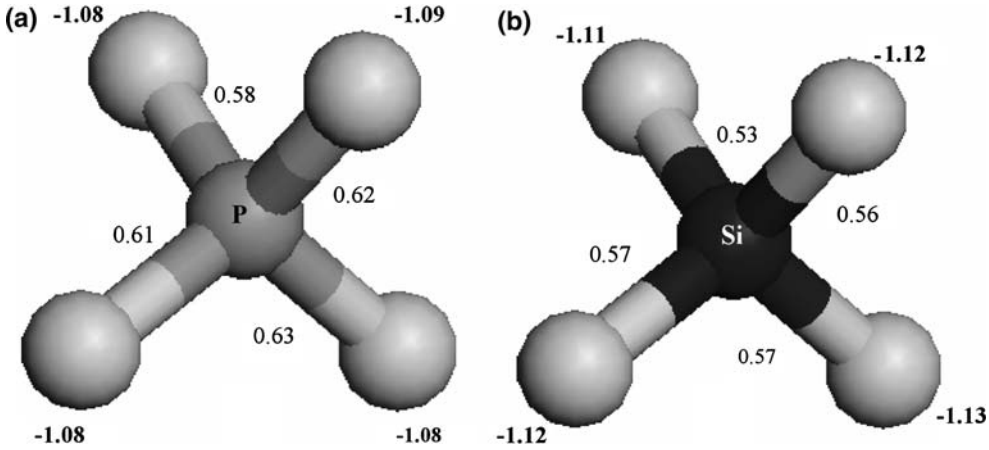

Fig. 4 Mulliken charges (bold) for oxygen atoms in (**a**) PO_4 and (**b**) SiO_4. Bond orders are also given for the P–O and Si–O bonds, respectively

how these values *change* in different environments. A maximum spilling parameter of 0.97% was achieved which indicates the largest error in the projection of the total charge. For phase-pure HA, the averaged charges on the Ca, P and O ions were calculated to be 1.36 |e|, 2.28 |e| and –1.08 |e|, respectively. The P–O bond populations were found to be 0.62, 0.61, 0.58 and 0.63 electrons. When Si is substituted for P in the structure its charge was calculated to be +1.95 |e| compared to +2.43 |e| in bulk silicon oxide (cristobalite). Additionally, the charges on the four neighbouring oxygen atoms decreased from an average of –1.08 |e| to an average of –1.12 |e| as shown in Fig. 4.

These results indicated that the substitution induced a small amount of charge transfer with the oxygen ions becoming slightly more negatively charged. The Si–O bond populations were found to be 0.56, 0.57, 0.53 and 0.57 electrons indicating a weakening of the oxygen bonds surrounding the Si impurity compared to the oxygen bonds around the equivalent phosphorus atom. On average the Si–O bond length is 5.53% longer than the P–O bond in the same position.

5 Conclusions

Density functional, plane-wave, pseudopotential calculations have been performed on silicon-substituted hydroxyapatite (SiHA). Formation energies have been determined for the substitution of a phosphorus atom by a silicon atom in each of the six phosphate groups of the unit cell in turn. It is found that the co-removal of a hydroxyl group to maintain charge neutrality is energetically favourable and the calculated cell volumes for the single silicon substitutions agree extremely well with experimental observation. The results support the belief that the incorporation of silicon into the lattice is accompanied by the formation of hydroxyl vacancies. The substitution of a second silicon atom in the unit cell is found to be almost as energetically favourable as the first (and on one site more favourable) and there can be an attractive interaction between the two Si_P defects when they are closely separated. However, experimental observation suggests that for this concentration of silicon a phase transformation to a different structure occurs which, because of the imposed boundary conditions, could not be accessed in the calculations. Despite this, it is clear from the study that low concentrations of Si (<3 wt%) can be readily substituted into the HA lattice. The density of states of the SiHA indicates that new states are introduced deep into the valence band and the band gap decreases by 1.6 eV compared to phase-pure HA. No new states are introduced into the band gap indicating that the Si incorporation does not make the material inherently electrically active. A Mulliken population analysis indicates that silicon substitution has only a small effect on the neighbouring ionic charges.

Acknowledgments Helen Chappell would like to thank the EPSRC and ApaTech Ltd for supporting this project. The calculations were performed using the CCHPCF (Cambridge) and HPCx (Daresbury) computing facilities. The authors would like to acknowledge useful discussions with Dr Alex Porter and technical advice from Dr Phil Hasnip.

References

1. N. H. DE LEEUW, *Chem. Commun.* **17** (2001) 1646
2. S. M. REA, S. M. BEST and W. BONFIELD, *J. Mater. Sci. Mater. Med.* **15**(9) (2004) 997
3. A. PEETERS, E. A. P. DE MAEYER, C. VAN ALSENOY and R. M. H. VERBEECK, *Phys. Chem. B* **101** (1997) 3995
4. T. KOBAYASHI, S. NAKAMURA and K. YAMASHITA, *J. Biomed. Mater. Res.* **57** (2001) 477
5. N. H. DE LEEUW, *Phys. Chem. Chem. Phys.* **4** (2002) 3865

6. N. H. DE LEEUW, *J. Phys. Chem. B* **108**(6) (2004) 1809
7. I. R. GIBSON, S. M. BEST and W. BONFIELD, *J. Biomed. Mater. Res.* **44** (1999) 422
8. H. F. CHAPPELL, MPhil Dissertation, University of Cambridge (2003)
9. S. WEN and Q. LIU, *Microscopy Res. Tech.* **40** (1998) 177
10. A. E. PORTER, S. M. BEST and W. BONFIELD, *Key Eng. Mat.* **240–2** (2003) 505
11. A. E. PORTER, N. PATEL, J. N. SKEPPER, S. M. BEST and W. BONFIELD, *Biomaterials* **24** (2003) 4609
12. I. R. GIBSON, S. M. BEST and W. BONFIELD, *J. Am. Ceram. Soc.* **85**(11) (2002) 2771
13. I. R. GIBSON, K. A. HING, P. A. REVELL, J. D. SANTOS, S. M. BEST and W. BONFIELD, *Key Eng. Mater.* **254–256** (2002) 203
14. E. M. CARLISLE, *Science* **167** (1970) 179
15. C. M. BOTELHO, M. A. LOPES, I. R. GIBSON, S. M. BEST and J. D. SANTOS, *J. Mater. Sci. Mater. Med.* **13** (2002) 1123
16. N. PATEL, S. M. BEST and W. BONFIELD, *J. Mater. Sci. Mater. Med.* **13** (2002) 1199
17. M. JIANG, J. TERRA, A. M. ROSSI, M. A. MORALES, E. M. BAGGIO SAITOVITCH and D. E. ELLIS, *Phys. Rev. B* **66** (2002) 224107
18. M. C. PAYNE, M. P. TETER, D. C. ALLAN, T. A. ARIAS, J. D. JOANNOPOULOS, *Rev. Mod. Phys.* **64**(4) (1992) 1045
19. M. D. SEGALL, P. J. D. LINDAN, M. J. PROBERT, C. J. PICKARD, P. J. HASNIP, S. J. CLARK and M. C. PAYNE, *J. Phys. Condens. Matter* **14** (2002) 2717
20. D. VANDERBILT, *Phys. Rev. B* **41** (1990) 7892
21. H. J. MONKHORST and J. D. PACK, *Phys. Rev. B* **13**(12) (1976) 5188
22. J. PERDEW, K. BURKE and M. ERNZERHOF, *Phys. Rev. Lett.* **77**(18) (1996) 3865
23. W. H. PRESS et al. Numerical recipes (Cambridge University Press, 1989)
24. Materials Studio 3.1, Accelrys
25. S. M. BEST, W. BONFIELD, I. R. GIBSON, L. J. JIA and S. J. D. DA SILVA, *Silicon-substituted apatites and process for the preparation thereof* (August 9, 1999), Patent Number: 6,312,468
26. A. E. PORTER, PhD Thesis, University of Cambridge (2003)
27. M. D. SEGALL, C. J. PICKARD, R. SHAH and M. C. PAYNE *Mol. Phys.* **89** (1996) 571

Since submitting our paper we have become aware of another very recent DFT paper on SiHA which uses localised orbitals and confirms that the OH vacancy is a stable charge compensation mechanism: R. Astala, L. Calderin, X. Yin and M. J. Stott, Chem. Mat. 18, 413 (2006).